Final Revised version 2004JB003230R– completed ~~22/05/2006~~2006 December 07

25 years of geodetic measurements along the Tadjoura-Asal rift system, Djibouti, East Africa.

Christophe Vigny[1], Jean-Bernard de Chabalier[2], Jean-Claude Ruegg[2], Philippe Huchon[3], Kurt L. Feigl[4], Rodolphe Cattin[1], Laike Asfaw[5], Khaled Kanbari[6].

[1]Laboratoire de Géologie, Ecole Normale Supérieure (ENS), CNRS, Paris, France

[2]Institut de Physique du Globe (IPGP), Paris, France

[3]Laboratoire de Tectonique, Université Pierre et Marie Curie-Paris_6 & Institut Océanographique, Paris, France

[4]Centre National de Recherche Scientifique (CNRS) Toulouse, France

[5]Addis Observatory, Department of Geophysics, Addis Ababa University, Addis Ababa, Ethiopia

[6]Department of Geosciences, University of Sana'a, Sana'a, Yemen

Abstract

Since most of Tadjoura-Asal rift system sits on dry land in the Afar depression near the triple junction between the Arabia, Somalia and Nubia plates, it is an ideal natural laboratory for studying rifting processes. We analyze these processes in light of a time series of geodetic measurements from 1978 through 2003. The surveys used triangulation (1973), trilateration (1973, 1979 and 1981 to 1986), leveling (1973, 1979, 1984-1985, and 2000), and the Global Positioning System (GPS, in 1991, 1993, 1995, 1997, 1999, 2001, and 2003). A network of about 30 GPS sites covers the Republic of Djibouti. Additional points were also measured in Yemen and Ethiopia. Stations lying in the Danakil block have almost the same velocity as Arabian plate, indicating that opening near the southern tip of the Red Sea is almost totally accommodated in the Afar depression. Inside Djibouti, the Asal-Ghoubbet rift system accommodates 16±1 mm/yr of opening perpendicular to the rift axis, and exhibits a pronounced asymmetry with essentially null deformation on its southwestern side and significant deformation on its northeastern side. This rate, slightly higher than the large-scale Arabia-Somalia motion (13 ± 1 mm/yr), suggests transient variations associated with the relaxation processes following the Asal-

Ghoubbet seismo-volcanic sequence of 1978. Inside the rift, the deformation pattern exhibits a clear two-dimensional pattern. Along the rift axis, the rate decreases to the northwest, suggesting propagation in the same direction. Perpendicular to the rift axis, the focus of the opening is clearly shifted to the northeast, relative to the topographic rift axis, in the "Petit Rift", a rift-in-rift structure, containing most of the active faults and the seismicity. Vertical motions, measured by differential leveling, show the same asymmetric pattern, with a bulge of the northeastern shoulder. Although the inner floor of the rift is subsiding with respect to the shoulders, all sites within the rift system show uplift at rates varying from 0 to 10 mm/yr with respect to a far-field reference outside the rift.

Introduction

The Afar depression, at the triple junction between Arabia, Somalia, and Nubia, is actively deforming by continental stretching, rifting, and volcanism. Here, the three extensional structures of the Sheba Ridge, the Red Sea Ridge, and the East African Rift join in a complicated geometry. Both the Red Sea Ridge and Sheba Ridge have been propagating for the last 30 Myr, toward the south and west, respectively. Yet they penetrate into the Afar depression, rather than connecting directly through the Straits of Bab el Mandeb. Consequently, the recent tectonic action there focuses around a set of disconnected, but overlapping, propagating rift segments that have created a complex network of normal faults (e.g., *Huchon et al.* [1991]; *Manighetti et al.* [1997]). To better understand the kinematics and the processes taking place in this area, we use geodetic measurements to characterize the deformation at three scales defined by different geophysical objects: the plates (distances ~ 1000 km), tectonic regions (between ~1000 km and ~10 km), and rift segments (~10 km).

At the scale of the plates, the existing long-term kinematic models disagree markedly. The conventional NUVEL-1A model considers Africa as a single plate to predict divergence between Africa and Arabia at a rate of about 16 mm/yr and N28°E in azimuth at the southern tip of the Red-Sea [*Demets et al.*, 1994]. Separating Africa into two plates, Somalia and Nubia, *Jestin et al.* [1994] propose a similar relative velocity: 17 mm/yr at azimuth N30°E. Yet the rate of Arabia-Somalia motion varies along the Sheba Ridge from 22 mm/yr at the horn of Africa to 17 mm/yr at the entrance to the Gulf of Tadjoura [*DeMets et al.*, 1994]. For the East African Rift (EAR) that splits Africa into Somalia and Nubia, estimates of the divergence rate also vary considerably: 1 mm/yr [*Asfaw et al.,* 1992], 5 mm/yr [*Jestin et al.*, 1994], or 6 mm/yr [*Chu and Gordon*, 1999].

In contrast, recent GPS measurements in this area clearly differ from plate kinematic predictions. Different geodetic studies show that the plate rates consistent with the GPS observations are about 30% slower than the NUVEL-1A estimates for Arabia-Eurasia [McClusky et al., 2000, 2003; Sella et al., 2002; Vernant et al., 2004; Vigny et al., 2006] and Arabia-Somalia [Fernandes et al., 2003; Vigny et al., 2006]. These results suggest that spreading in the Red Sea and the Gulf of Aden, and thus the convergence rate between Arabia and Eurasia, has slowed during the last 3 Ma [*Vigny et al.,* 2006].

At the smaller, regional scale of the Afar Depression, the complexity of the active fault and rift systems leads to various interpretations. Tectonic observations and paleomagnetic declinations suggest that the Danakil and Ali Sabieh blocks are both rotating [*Sichler et al.,* 1980; *Courtillot et al.,* 1980; *Souriot and Brun*, 1992; *Manighetti et al*., 1998]. The rotations can be understood as a consequence of rift propagation, either as “oceanic micro-plates” [*Acton and Stein*, 1991] or “continental bookshelf faulting” [*Tapponnier et al*., 1990; *Sigmundsson et al.,* 1992; *Manighetti et al.,* 1998; 2001a and b]. Implicit in all these models is the idea that the deformation transfers from one rift to another and therefore evolves in space and in time. This complication makes evaluating these models by comparing their predictions to quantitative geodetic measurements quite challenging. Confronting long-term, plate-scale models with short-term regional geodetic surveys requires accounting for the dynamics of the underlying processes.

In this paper, we focus on the boundary between the Arabia plate and the Somalia where Sheba Ridge enters into the Afar depression. This narrow, WNW-trending zone of active volcanism and tectonics includes Maskali transform fault, the Tadjoura rift and the Asal-Ghoubbet rift. To the NW, it links to the Mak'arassou fault system and the Manda Inakir rift (Figures 1 and 2). The Asal-Ghoubbet rift is special because we can observe it on dry land to better understand slow-spreading ridges in oceanic lithosphere. Reconstructing the edifice of Fieale volcano indicates an average spreading rate of 17 to 29 mm/yr over the last 87,000 to 150,000 years at an azimuth of N40°E ± 5 that is consistent with plate kinematic estimates [*de Chabalier and Avouac*, 1994]. The rate of opening at the rift, however, is not constant, as evidenced by a rifting event in 1978. Then, a swarm of earthquakes (two of which had magnitude near 5) reactivated several normal faults, producing a total of 2 m of extension, during a week of volcanic activity at a new eruptive center (e.g., *Abdallah et al.* [1979]). The geodetic measurements performed during the years following this sequence confirm that strain rates as fast as ~10^{-6}/yr concentrate in the Asal rift [*Ruegg et al.,* 1979; *Ruegg and Kasser*, 1987]. All these observations indicate that the Asal-Ghoubbet rift accommodates most of the present-day motion between Arabia and Somalia. Outside the rift, no direct measurements have yet been published to determine which other structure might accommodate any remaining motion.

In this paper we present 12 years of GPS campaign measurements in Djibouti, Yemen, and Ethiopia. At the regional scale, we discuss the strain concentrated in the active rifts spanned by the GPS network. At the local scale, we use over 25 years of geodetic data to argue that transient rifting episodes like the one in 1978 at Asal are the dominant process in accommodating the motion across this plate boundary. Finally, we confirm this interpretation by considering the vertical displacements measured by GPS and leveling.

GPS data analysis

In November 1991, the first GPS observations were performed in Djibouti and the neighboring parts of Yemen and Ethiopia [Ruegg et al., 1993]. A small subset of this network was surveyed again three times in 1993, once in 1995, and once in 1997. More complete surveys of the rift network were performed in 1999, 2001, and 2003 (Table S1). The points in Yemen were measured for the second time in 2001, ten years after the first survey. All sites were measured using a mix of Ashtech and Trimble dual-frequency receivers equipped with different kinds of antennas (see Table S1 for details) During all campaigns, three points (Arta in Djibouti, Sana'a in Yemen, and Addis Abbeba in Ethiopia) were measured continuously in 24-hour sessions. Other sites in Djibouti were measured for 6 to 24 hours per day over 1 to 6 days (Table S1).

We reduce these data in 24-hour sessions to daily estimates of station positions using the GAMIT software [*King and Bock*, 2000], choosing the ionosphere-free combination, and fixing the ambiguities to integer values. We use precise orbits from the International GPS Service for Geodynamics (IGS) [*Beutler et al*., 1993]. We also use IGS Tables to describe the phase centers of the antennae. We estimate one tropospheric delay parameter per station every 3 hours. The horizontal components of the calculated relative position vectors are precise to within a few millimeters for pairs of stations less than 150 km apart, as measured by the root mean square (RMS) scatter about the mean.

In the second step, we combine the daily solutions using the GLOBK software [*Herring et al.*, 1990] in a "regional stabilization" approach [*McClusky et al.,* 2000]. To define a consistent reference frame for all epochs, we include tracking data from the permanent stations of the International GPS Service (IGS) [*Neilan*, 1995]. The number of IGS stations around our study area available at the time of our campaigns was 4 in 1991 but increased to 42 in 2003. These fiducial stations are also included in the daily global GAMIT solutions from the IGS data center at Scripps, including more than 200 stations spread all over the globe. We combine all these daily solutions using Helmert-like transformations to estimate translation, rotation, scale and Earth orientation parameters (polar motion and UT1 rotation). This "stabilization" procedure defines a reference frame by minimizing, in the least-square sense, the departure from the prior values determined in the International Terrestrial Reference Frame (ITRF) 2000 [*Altamimi et al*., 2002]. This procedure estimates the positions and velocities for a set of 22 well-determined stations in and around our study area. The misfit to these "stabilized" stations is 2.8 mm in position and 1.6 mm/yr in velocity. More details about this solution and velocity residuals can be found in *Vigny et al.* [2006].

Horizontal velocities

This procedure leads to horizontal velocities with respect to ITRF2000 (Table 1). We compute velocities relative to the Somalian plate by using the angular velocity of this plate (48.12°N, -97.75°W, 0.329°/Myr) given by *Vigny et al.* [2006]. In this reference frame, three sites in southern Djibouti (CBL0, LLL0, GOR0) located far from the rift axis and supposedly on the Somalian plate, show velocities smaller than 1 mm/yr (Figures 1, 2, Table 1). Three more stations immediately south of the Asal-Tadjoura rifts (ARO0, QQQ0, and CCC0) also exhibit little motion, whereas site III0 is a notable exception (Figure 2, Table 2). Therefore we chose to show all velocities in this reference frame, i.e. with respect to the Somalia plate. This choice has the advantage of highlighting the deformation in and around the Asal rift because the velocities of sites on the stable area south of it appear as short, insignificant arrows.

Far-field velocities

In this Somalia-fixed reference frame, the residual velocity in Addis Abebba (ADD1), west of the East African Rift (EAR), is 4 mm/yr (±1 mm/yr at 1-σ), oriented roughly West (Figure 1 and Table 1). The amplitude of this residual vector depends on the angular velocity estimated for the Somalia plate. Different solutions give velocities between 3 and 6 mm/yr that are consistent within 95 percent confidence. Their azimuths fall between West and North-West, roughly perpendicular to the EAR trace at this latitude. Therefore, we conclude that our value of 4 mm/yr ± 2 is an upper bound for the EAR opening rate just south of the Afar depression.

The stations in Yemen (DHAM, HODD, JNAR, SANA) move together as a coherent block that represents a part of the Arabia plate with very little internal deformation (Figure 1). The azimuth of their average velocity (N25° ± 5) is compatible with the orientations of Gulf of Aden transform faults used to determine the NUVEL-1 model [*Demets et al.,* 1990]. On the contrary, their mean opening speed (13 ± 2 mm/yr) is 30% slower than the Nuvel-1A rate [*Vigny et al.*, 2006]. This definition of the Arabia plate implies that two stations located at the southern tip of the Danakil block (TDJ0 and RSB0) are close to having "Arabian" velocities (Figure 1). Their residual motion with respect to the four stations in Yemen is less than 2 mm/yr. This confirms that the opening rate of the Red Sea at this latitude is negligible, which is not surprising given the absence of magnetic anomalies on the sea floor there. Therefore, we conclude that most, and possibly all, of the present day opening is accommodated west of the "Danakil block" represented by RSB0 and TDJ0 (Figure 1).

With respect to the African plate defined in *Vigny et al.* [2006] (50.48°N, -82.01°E, 0.265°/Myr), the motion of these two points (RSB0 and TDJ0) is 15 ± 2 mm/yr at N54±6°. Assuming that the Danakil block rotates about a pole near its northern end (at 16°N, 40°E), we find an angular velocity of 1.6 ± 0.1 °/Myr for the Danakil block. This spin rate agrees with the paleomagnetic estimate of 10.7° ± 4° over 7 Ma, which gives an average rate of 1.5 ± 0.6 °/Myr or 26 ± 10 µrad/yr [*Manighetti et al.*, 2001a, *Besse and Courtillot*, 1991]. Therefore, we conclude that the spreading between Arabia and Africa at this latitude, has been taking place west of the "Danakil block", i.e. along the deformation zones of the Afar depression, for at least the last 7 Ma.

Djibouti and the Gulf of Tadjoura

Deformation along the northern side of the Gulf of Tadjoura (Figure 2) exhibits a clear gradient from 16 mm/yr on the north-eastern Asal-Ghoubbet rift shoulder to 11 mm/yr in the Danakil block (RSB0, TDJ0). Stations FFF0, MMM0, and RRR0, lying at the same distance from the Asal-Ghoubbet rift axis, display a coherent velocity of 16 ±1 mm/yr and N45° ± 8° on average. We are particularly confident in the velocity of point FFF0 since it has been measured four times during the last 12 years with a remarkably stable time series. Point PPP0, located at intermediate distance between the "Danakil-Arabian" area and the rift shoulder, has a transitional velocity of 15 ± 3 mm/yr with the same azimuth.

On the southwestern side of the Asal-Ghoubbet rift, we observe no significant velocity gradient between the southern rift shoulder (CCC0 or QQQ0) and the Somalia plate as we have defined it. Yet this interpretation is subject to two caveats: First, there are no GPS sites between GOR0 in the far field and the southern rift shoulder. Second, the motions of QQQ0 and III0 differ markedly: the former has a small insignificant residual velocity, while the latter has an unexpected and probably erroneous high velocity of 10 mm/yr. Despite these caveats, we infer an asymmetry in the extensional deformation pattern between the northern part and the southern part of the Asal-Ghoubbet rift. This asymmetry is also apparent in the vertical deformation recorded by the topography, the faults activated during the 1978 sequence, and the way individual faults shift their activity to the northeast [*Ruegg et al.*, 1990; *Stein et al.*, 1991; *Ruegg and Kasser*, 1987].

All these results confirm that Asal-Ghoubbet rift accommodates most of (indeed, more than) the present-day motion of Arabia-Somalia expected during the 12-year observation period. In particular, the dense GPS network along the coast of the Gulf of Tadjoura shows no measurable deformation, either within the Tadjoura rift or on the faults between the Tadjoura and Asal rifts. Nor do we see any evidence for slip or creep on the active Gaggade-Hanle fault system, southwest of the Asal rift. Accordingly, we infer that the faults there are locked during this time interval.

Why, then, is the extension rate of 16 mm/yr across the Asal rift some 50% faster than the Arabia-Somalia plate motion? The most probable explanation involves the transient processes that took place in the rift following the 1978 seismo-volcanic sequence, when up to 1.9 m of extension were measured across the rift [*Ruegg et al.,* 1979]. During the following decade, extension at a rate of 60 mm/yr has been measured across the inner rift fault system that was activated during the 1978 sequence [*Ruegg and Kasser,* 1987]. After 1987, this rate decreased to about 1 cm/yr, slower than the far-field rate imposed by large-scale plate tectonics (Figure 3). That the rate of opening changed drastically in the 6 years following the 1978 rifting event suggests two possible interpretations.

In the first interpretation, the opening continued at a constant rate of 53 mm/yr from 1980 through 1986 [*Ruegg and Kasser*, 1987]. Then the rate of opening slowed abruptly to 13 mm/yr, close to the geologic plate rate, suggesting that driving processed ceased abruptly. Although this model, with three parameters (two slopes and an intercept), is the simplest possible description of the time series shown in Figure 3, it does not appear to be compatible with other geophysical observations. In particular, there is no suggestion of a similar change in the seismicity around 1986. Nor do field observations suggest that the seismo-volcanic activity that “boiled over” in the 1978 crisis continued to simmer for the next 8 years. Fresh lava, for example, was observed only in 1978.

The second interpretation involves post-seismic relaxation in the years following the 1978 rifting event. One simple model for this is a 1-dimensional Elsasser formulation, consisting of an elastic layer over a viscous layer, as suggested for a similar rifting event in 1974 at Krafla, Iceland [*Foulger et al*., 1992; *Sigmundsson*, 2006]. The upper, elastic layer has thickness h and rigidity μ. The lower, viscous layer has Newtonian dynamic viscosity η and thickness b. This configuration of geometry and rheology leads to the diffusion equation with a stress diffusivity κ. Accordingly, the pulse of stress produced by the initial dike injection diffuses away from the axis. For a dike of half-width U_0, intruded into the elastic layer at time $t = 0$, the resulting horizontal displacement is

$$u(x,t) = U_0 \operatorname{erfc} \frac{x}{2\sqrt{\kappa t}} \qquad (1)$$

where x is the distance from the rift, and *erfc* is the complementary error function [*Foulger et al.*, 1992]. Fitting the geodetically observed values in Figure 3, we find an initial half-opening of $U_0 = 0.4$ m and a stress diffusivity of $\kappa = 0.015$ m^2/s. The value of the full initial opening $2U_0$ estimated from fitting the data is about half of the 1.9 meters of opening measured in 1978 [*Abdallah et al.* [1979]. The stress diffusivity κ may be interpreted as the product of the two thicknesses divided by a time scale τ

$$\kappa = \frac{hb}{\tau} \qquad (2)$$

In the case of a Poisson solid with a Poisson ratio of ¼, the time scale τ is proportional to the ratio of the viscous effects to the elastic effects

$$\tau = \frac{3\eta}{8\mu} \qquad (3)$$

Having established that velocities in the area change with time, one might worry that velocities inferred from campaign GPS measurements represent only an average on the time interval between two epoch measurements. In this case, comparing measurements made at different epochs at different locations might cause aliasing. However, time series of the distance across the rift axis from EP00 DF00 shows an approximately constant rate between 1987 and 2003 (Figure 3). In other words, the transient has decayed sufficiently so that it can be fit reasonably well by a constant linear rate for the time span of our GPS campaigns (1991-2003). The misfit is less than 2 mm/yr, consistent with the uncertainties in the GPS velocity estimates.

The Asal Rift

Figure 4 shows the details of the deformation field inside the Asal rift, as measured by the relative velocities of about 20 points throughout the rift valley (Figure 4). As at the larger scale, the rate of opening observed on the NE shoulder of the Asal rift is very coherent, with a constant rate of 16 mm/yr ±1 at azimuth N45° ± 8° for the line through stations FFF0, GM00, MMM0, and RRR0. These stations move together as a unit that we call a “panel” that can be defined by the geomorphic expression of the active faults bounding it.

Nearer the rift axis, on the next panel to the southwest, we observe a marked variation along the strike of the panel: 16 mm/yr at BY00, 13 mm/yr at DF00, 10 mm/yr at CF00 and 6 mm/yr at AS00. This last line of points is located at the northern border of the “Petit Rift”, a rift-in-rift structure with a dense network of faults, open fissures, and cracks that appears to be the most active part of the Asal rift. This line of points also marks the northern boundary of the set of faults that slipped during the 1978 seismo-volcanic sequence. The GPS stations’ velocities decrease from SE to NW, following the shape of the “Petit Rift” that terminates just southeast of station CF00 [*deChabalier and Avouac,* 1994]. This rate variation indicates propagation from SE to NW, as suggested from geomorphologic observations [*Manighetti et al.*, 1998]. This propagation appears to be shallow, probably less than 3-4 km deep, because its effects do not reach the previous panel: FFF0, GM00, MMM0, and RRR0 move with the same velocity.

On the southwestern side of the rift, the velocity field is not so clear, mainly because stations (HM00, FG00, GK00, and HX00) have large uncertainties that reflect infrequent measurements. Nonetheless, we can define a shoulder panel including the stations HX00, FG00, and HM00 with speeds of 1 to 7 mm/yr, and another panel including stations GK00, EP00, and LS00 with a velocity of about 5 to 8 mm/yr. Points HD00 and SN00, located close to the rift axis, show rates of 4 and 9 mm/yr with respect to the Somalian plate, respectively. The general pattern on the southwest side of the rift indicates a small, gradual increase in velocity from the southwestern shoulder to the axis.

To visualize the high strain rates concentrated in the Asal rift, we project the velocities onto four profiles striking 45E°, perpendicular to the rift axis (Figure 5). The average strain rate is 1 mm/yr/km (or 3×10^{-14} s^{-1}). Most of the points on the NE side of the rift axis move faster than this average strain rate, while those in the SW part move more slowly. This signature becomes clearer, if we neglect stations HX00 and AS00 (profile 4) that sit near Lake Asal and are therefore perturbed by the along-strike variation due to the northwestward propagation of the rift. Indeed, this signature is expected from the diffusive model. The curve in Figure 5 shows the velocity calculated using the 1-dimensional Elsasser model (equation 4 in *Foulger et al.* [1992]) with the diffusivity κ and initial opening U_0 estimated above, an elapsed time of 19 years between the crisis in 1978 and the mean date (1997) of our GPS campaigns, and located at a distance of x = 1 km northeast of the main rift axis. The deformation concentrates to the NE of the geomorphologic long-term rift axis such that the highest velocity gradient occurs in the "Petit Rift" between stations SN00 and DF00-BY00 (Figure 5). This area coincides with the maximum of fault breaks observed during the 1978 sequence [*LeDain et al.,* 1979; *Ruegg et al.,* 1979] and with the present-day seismicity, which is mostly located in the northern part of the rift [*Doubre et al.,* 2005]. Furthermore, the fastest points, showing the location of the post-seismic diffusive pulse in 1997, fall 3 to 5 km away from the "Petit Rift" axis on the northeast side. However, the major limitation of this simple model lies in its symmetry with respect to the rift axis, which causes a large misfit at station CCC0 on the southwest side. Therefore, we conclude that this model is a reasonable a first-order approximation. A more sophisticated, second-order approximation should account for geometric complexities such as creep on dipping faults.

Rates of vertical motion

Conditions in the Asal rift are good for measuring the vertical component of the tectonic deformation field. Some points of our network have been measured many times over a 12-year interval. Measurement campaigns were usually conducted at the same time of the year, during winter. Relative distances between points are small. Finally, almost all points are located on good, solid outcrops, clearly attached to the bedrock. The floor of the innermost valley in the rift could be subsiding as fast as 10 mm/yr with respect to the shoulders. Accordingly, we expect the ratio of tectonic signal to geodetic measurement uncertainty to be larger than unity.

Intermediate- scale GPS

Selecting stations measured at least four times, we define a subset of points around the rift with vertical velocities determined to within ± 5 mm/yr (Figure 6). Stations located far from the rift (RSB0 and TDJ0 on the north side and CBL0 and LLL0 on the south side) show no motion to within ± 2-3 mm/yr. They represent a stable reference frame for analyzing vertical motions in the rift. Near the eastern tip of the rift, stations RRR0 and QQQ0 also show small, but marginally significant, velocities of +2 to +3 mm/yr upward with respect to the far-field reference. Points located further west on the shoulders of the rift show a fairly symmetric and significant uplift between 6 and 11 mm/yr. From these values, we can estimate an average uplift value of 8 ± 3 mm/yr, and locate the maximum uplift in the central part of the rift, midway between Lake Asal and Ghoubbet Al Kharab.

Small scale: leveling and GPS inside the rift

To measure vertical motions over short distances, classical spirit leveling is usually more appropriate than GPS. With care, one can limit the drift of the technique to less than one part per million (1 mm per km). It is therefore possible to detect millimeter-sized vertical displacements between two leveling surveys made on the same line at different epochs. A precise leveling line with about 200 marks was established in 1973 along 100 km of the road crossing the rift. The central part of this line was measured for the second time in 1979, after the Ardoukoba seismo-volcanic crisis [*Abdallah et al.*, 1979; *Ruegg et al.*, 1979], and again in the winter of 1984–1985 [*Ruegg and Kasser*, 1987]. Over this 6-year interval, uplift rates as fast as 10 to 15 mm/yr were detected. The pattern is similar on both sides of the rift axis. The inner floor subsides with respect to the shoulders, but uplifts with respect to the far field.

This leveling line was measured for the fourth time in 2000. The 1985-2000 comparison gives vertical rates over a 15-year period (Figure 7). The inferred pattern of deformation shows both similarities and differences with the 1978-1985 one. Both intervals show the same pattern of uplift of the rift shoulders and relative subsidence of the inner floor. Yet the rates for the 1985-2000 interval are 50% slower than those for 1978-1985, indicating that the post-seismic transient after the 1978 crisis is still decaying. The peak around km 32 in the inner rift floor appears to represent the same two-dimensional effect as seen in the horizontal velocities. Since this portion of the leveling line runs parallel to the rift axis, the uplift varies as a function of position along strike, probably reflecting the same propagation process. The points on the NE side (after km 45) differ from previous measurements. They suggest that the uplifting area was wider after 1985 than before, consistent with the diffusive Elsasser model.

This finding is consistent with recent INSAR results obtained for the 1997-2003 interval [*Doubre et al.*, 2005]. Yet this finding should be taken with some caution. Systematic errors in the levelling measurements could conceivably produce a systematic pattern. The change in height at the end of the line is only 75 mm with respect to the starting point 65 km away. The overall trend is only slightly more than 1 mm/km, close to the measurement uncertainty. Unfortunately, the line was measured in a forward run only, preventing us from using the misclosure to estimate the uncertainty. Also, the measurements stopped short of the end point of the 1973 line in the far field. Consequently, we must rely on the internal error analysis to evaluate the precision of this leveling profile. The lines of sight were kept short: 15 m on average and very seldom longer than 30 m (Figure S1a). Forward and backward lines of sight were symmetric within 10 to 20% to cancel out any asymmetric behavior of the leveling instrument (Figure S1b). We avoided as much as possible hitting the surveyor's pole at low heights, too close to ground level where atmospheric distortions are largest (Figure S1c). Finally, the ten small loops of length shorter than 1 km all closed to within 1 mm, without any systematic trend (Figure S1d). Considering all these reasons together, we can exclude systematic errors as the cause of the uplift observed on the northeast side of the rift.

However, a change of height does not necessarily imply a change of topographic elevation. It could be that the local geoid changed over the 15-year time span between the two leveling surveys. Indeed, some indication that this may have occurred comes from gravity measurements conducted in the area in 1999 [*Ballu et al.,* 2003]. These measurements suggest that the gravitational acceleration decreased in this area between 1985 and 1999. Such a change could be interpreted in terms of uplifting the benchmarks, decreasing the density of the rocks below them, or some combination of the two.

We can glean a little more information from a two-dimensional comparison with the vertical velocities for the GPS stations inside the rift. Again selecting stations measured at least four times, we see some coherent signal (Figure 8). The results are similar if we select three occupations over a minimum of eight years. First of all, this map view highlights the two-dimensional distribution of the vertical motions. Far from being a straight line across the rift, the leveling line meanders around faults and cliffs and samples the uplift at different locations along the rift axis. Thus the signal on the rift inner floor varies along its strike: less than 1 mm/yr near the Ghoubbet shore but close to 5 mm/yr some 5 km inland. Second, there is a general good agreement between the GPS and leveling estimates on the NE side of the rift. Both techniques see the shoulder uplifting at 5 to 7 mm/yr (GM00 and DF00). The next panel, represented by station CF00, is rising by only 4 mm/yr with respect to the valley floor, but subsiding with respect to the shoulder. The inner rift floor is clearly subsiding, with 2 to 4 mm/yr in the "Petit Rift" (stations HD00 and SN00). Points on the other side of the rift axis, but close to the Ghoubbet have very small velocities (+2 mm/yr at EP00, –2 mm/yr at LS00). All these values are consistent with the leveling values, except GK00 and FG00 which have large uncertainties. They indicate the sum of two signals: a subsidence of the inner floor with respect to the shoulders and an inflation signal located in the middle of the rift. The SW side of the rift is different: GPS vectors indicate an uplift of the rift shoulder where the leveling returns to zero (HX00 and CCC0).

Conclusion

Vigny et al. [2006] have shown that the far-field plate rates estimated from GPS data acquired over the 12-year interval are 30% slower than predicted by plate-motion models based on the last several million years. Our estimate for the rate of opening across the Asal rift between Somalia and the Danakil block is 11 ± 1 mm/yr, based on ten GPS stations observed between 1991 and 2003. Clearly, the deformation pattern across this complex plate boundary is more complicated than supposed by classical plate tectonics, which neglects internal deformation within each plate.

The rifting event in 1978 created a significant transient in the deformation pattern. Over 25 years later, the inner rift is still opening at a rate faster than the far-field value. This observation can be mimicked to first order by a simple one-dimensional Elsasser model of an elastic layer over a viscous layer. For the 1978 Asal crisis in Djibouti, however, the estimated diffusivity is two orders of magnitude smaller than estimated for the 1974 Krafla crisis in Iceland [*Foulger et al.,* 1992]. The diffusivity measures the ratio of the product of the two thicknesses (or length scales) to the time scale. The time scale is the time between the rifting episode and the second geodetic survey, i.e. 19 years at Asal and 11 years at Krafla. One length scale is the distance from the rift axis to the fastest-moving point (at that time), 3 km at Asal, considerably shorter than the 25 km at Krafla. The diffusivity ratio for Asal with respect to Krafla is ~1/70, implying that the top elastic layer is at least an order of magnitude thinner beneath Asal and/or that the viscosity of the underlying substrate is at least an order of magnitude higher at Asal than at Krafla. Although these differences are qualitatively consistent with the tectonic settings of Djibouti and Iceland, their stark quantitative contrast suggests that the 1-dimensional analysis oversimplifies the problem somewhat.

A companion paper [*Cattin et al*., 2005], shows that a sophisticated model can fit the data better. For example, geometric considerations (multiple dipping, non-planar faults) and thermal effects (post-rifting cooling increases viscosity) lead to a complete 3-dimensional approach using numerical modeling. Such a model can explain the details of the inner rift deformation. For example, the geodetic data shown here suggest that the northern part of the rift zone accommodates more (some 70%) of the extension than the southern part.

Considering the amount of extension absorbed in the Asal rift during the 1978 sequence, the high post-seismic velocity, and the present-day velocity, we infer that the opening rate across the Asal rift will have to decrease significantly before the next such seismo-volcanic crisis can occur. The deformation recorded by the topography as well as the deformation recorded by the lake Asal Holocene markers, suggest that the recurrence time of such a crisis is about 120 to 300 yr [*Ruegg et al.*, 1990; *Stein et al*., 1991; *Manighetti et al.,* 1998]. However, the ongoing high rate and the fact that the rift and the flanks are both rising as a whole with respect to the far-field plate interiors are two indications that magma injection still prevails over extension as the active process driving the rifting today.

Acknowledgments. We are grateful to many people who participated in measurement campaigns, especially individuals from the “Observatoire d’Arta”. We thank J.-C. Delmont who was its director during the 1991 campaign and participated in the 1995 and 1999 campaigns. The leveling line was surveyed by A. Coulomb from IGN. Very special thanks to Moumin in Djibouti. The Afar geodetic program was sponsored by CNRS/INSU programs (Tectoscope-Positionnement, IDHYL, IT). We also appreciate the guidance of Peter Molnar, who read the manuscript twice and obtained a grant from NSF (OCE8916680) that boosted the 1991 campaign.

References

Abdallah, A., et al. (1979), Relevance of afar seismicity and volcanism to the mechanics of accreting plate boundaries, *Nature*, *282*, 17-23.

Acton, G. D., et al. (1991), Block rotation and continental extension: A comparison to oceanic microplate systems, *Tectonics*, *10*, 501-526.

Altamimi, Z., P. Sillardand C. Boucher (2002), ITRF2000: A new release of the International Terrestrial Reference frame for earth science applications, *J. Geophys. Res.,* SA 107 (B10): art. no. 2214.

Asfaw, L. M., et al. (1992), Recent inactivity in african rift, *Nature*, *357*, 447.

Ballu, V., et al. (2003), 1985-1999 gravity field variations across the asal rift: Insights on vertical movements and mass transfer, *Earth and Planetary Science Letters*, *208*, 41-49.

Besse, J., and V. Courtillot (1991), Revised and synthetic apparent polar wander paths of the African, Eurasian, North American and Indian plates, and true polar wander since 200 Ma, *J. Geophys. Res.,* 96, 4029-4050.

Beutler, G., J. Kouba, and T. Springer (1993), Combining the orbits of the IGS processing centers, in proceedings of IGS annalysis center workshop, *edited by J. Kuba*, 20-56.

Cattin, R., C. Doubre, J.B. de Chabalier, G. King, C. Vigny, J.P. Avouac and J.C. Ruegg (2005), Numerical modelling of quaternary deformation and post-rifting displacement in the Asal-Ghoubbet rift (Djibouti, Africa), *Earth Planet. Sc. Lett.*, 239, 352-367.

Courtillot, V., A. Galdeano and J.L. LeMouel (1980), Propagation of an accreting plate boundary: a discussion of new aeromagnetic data in the gulf of Tadjourah and southern Afar. *Earth Planet. Sci. Lett.*, 47, 144-160.

Chu, D., and R.G. Gordon (1999), Evidence for motion between Nubia and Somalia along the southwest Indian Ridge, *Nature*, 398, 64-67.

De Chabalier, J.B. and J.P. Avouac (1994), Kinematics of the Asal rift (Djibouti) determined from the deformation of Fieale volcano, *Science,* 265, 1677-1681.

DeMets, C., et al. (1990), Current plate motions, *Geophys. J. Int.*, *101*, 425-478.

DeMets, C., et al. (1994), Effect of the recent revisions to the geomagnetic reversal time scale on estimates of current plate motions, *Geophys. Res. Lett.*, *21*, 2191-2194.

Doubre, C., G. Peltzer, I. Manighetti and E. Jacques (2005), Eight years of surface deformation in the Asal-Ghoubbet rift (Afar depression) observed with SAR data, AGU fall meeting, abstract G42A04.

Fernandes, R.M.S., B.A.C. Ambrosius, R. Noomen, L. Bastos, M. Wortel, W. Spakman, and R. Govers (2003), The relative motion between Africa and Eurasia as derived from ITRF2000 and GPS data, *Geophys. Res. Lett., 30(16),* 1828, 2003, doi:10.1029/2003GL017089.

Foulger, G. R., C.-H. Jahn, G. Seeber, P. Einarsson, B. R. Julian and K. Heki (1992), Post-rifting stress relaxation at the divergent plate boundary in Northeast Iceland, *Nature*, 358.

Herring, T. A., et al. (1990), Geodesy by radio astronomy: The application of Kalman filtering to very long baseline interferometry, *J. Geophys. Res.*, *95*, 12,561-512,581.

Huchon, P., F. Jestin, J.M. Cantagrel, J.M. Gaulier, S. Al Khirbash and A. Gafaneh (1991), Extensional deformations in Yemen since Oligocene and the Afar triple junction, Annales Tectonicae 5 (2), 141-163.

Huchon, P., I. Manighetti, M. Al-Aawah, S. Al-Khirbash, L. Audin, O. Coulon, O. Dauteuil, H. Hebert, E. Jacques, K. Khanbari, S. Levasseur, A. Omar, T. Souriot, and P. Tapponnier (1995), Propagation of the Arabia-Somalia plate boundary in the western Gulf of Aden: new results of the 1995 TADJOURADEN cruise, in Rift sedimentation and tectonics in the Red Sea – Gulf of Aden region (abstract), Sana'a, Yemen.

Jestin, F., P. Huchon and J.M. Gaulier (1994), The Somalia plate and the East African Rift system: present day kinematics, Geophys. J. Int., 116, 637-654.

King, R. W., and Y. Bock (2000) Documentation for the GAMIT GPS software analysis version 9.9, *Mass. Inst. of Technol.*, Cambridge.

Le Dain, A.Y., B. Robineau, and P. Tapponnier (1979), Les effets tectoniques de l'évenement sismique et magmatique de novembre 1978 dans le rift d'Asal-Ghoubbet. *Bull. Soc. Géol. France* 7(6):817-822.

Manighetti, I. (1993), Dynamique des systèmes extensifs en Afar, *Paris 6 University Thesis*, 242pp, 1993.

Manighetti, I., P. Tapponnier, V. Courtillot, S. Gruszow and P.Y. Gillot (1997), Propagation of rifting along the Arabia-Somalia plate boundary: the gulfs of Aden and Tadjoura, *J. Geophys. Res.*,102 (B2), 2681-2710.

Manighetti, I., P. Tapponnier, P.Y. Gillot, E. Jacques, V. Courtillot, R. Armijo, J.C. Ruegg, and G. King (1998), Propagation of rifting along the Arabia-Somalia plate Boundary: into Afar, *J. Geophys Res.*103 (B3), 4947-4974.

Manighetti, I., P. Tapponnier, V. Courtillot, Y. Gallet, E. Jacques, and P.Y. Gillot (2001a), Strain transfer between disconnected, propagating rifts in Afar, *J. Geophys Res.,*106 (B7), 13613-13665.

Manighetti, I., G.C. King, Y. Gaudemer, C.H. Scholz, and C. Doubre (2001b), Slip accumulation and lateral propagation of active normal faults in Afar, *J. Geophys Res.,*106 (B7), 13667-13696

McClusky, S., et al. (2000), Global Positioning System constraints on plate kinematics and dynamics in the eastern Mediterranean and Caucasus, *J. Geophys. Res.*, 105, 5695-5720.

McClusky, S., R. Reilinger, S. Mahmoud, D. Ben Sari, and A. Tealeb (2003), GPS constraints on Africa (Nubia) and Arabia plate motions, *Geophys. J. Int., 155*, 126-138.

Neilan, R. (1995), The evolution of the IGS global network, current status and future aspects, in IGS annual report, edited by J.F. Zumberge et al., *JPL Publ.*, 95-18, 25-34.

Ruegg, J.C., J.C. Lépine, A. Tarantola, and M. Kasser (1979), Geodetic measurements of rifting associated with a seismovolcanic cris in Afar, *Geophys. Res. Lett.*, 6, 817-820.

Ruegg, J.C., and M. Kasser (1987), Deformation across the Asal-Ghoubbet Rift, Djibouti, uplift and crustal extension 1979-1986, *Geophys. Res. Lett.*, 14, 745-748.

Ruegg, J.C., F. Gasse and P. Briole (1990), Mouvements du sol holocènes dans le rift d'Asal à Djibouti, *C.R. Acad. Sci. Paris*, 310, 1687-1694.

Ruegg, J.C., P. Briole, K. Feigl, C. Vigny, M. Anis Abdallah, O. Bellier, P. Huchon, S. Al Khirbash, A. Laike, N. d'Oreye, and M. Prevot (1993), First Epoch Geodetic GPS Measurements Across the Afar Plate Boundary Zone. *Geophys. Res. Lett.*, 20, 1899-1902.

Sella, G.F., T. H. Dixon, and A. Mao (2002), REVEL: a model for recent plate velocities from space geodesy, *J. Geophys. Res.*, *107* (B4), 10.1029.

Sichler, B. (1980), La bielette danakile: un modèle pour l' évolution géodynamique de l'Afar, *Bull. Soc. Géol. Fr.*, 6, 925-933.

Sigmundsson, F. (2006), Iceland Geodynamics: Crustal Deformation and Divergent Plate Tectonics, 228 pp., Springer, Berlin.

Sigmundsson, F., P. Einarsson, R. Bilham (1992), Magma chamber deflation recorded by the Global Positioning System, the Hekla 1991 eruption, *Geophys. Res. Lett.*, 19(14) 1483-1486.

Souriot, T., and J.P. Brun (1992), Faulting and block rotation in the Afar triangle East Africa: the Danakil crank arm model. *Geology*, 20, 911-914.

Stein, R.S., Briole, P., Ruegg, J.C., Tapponnier, P. and F. Gasse (1991). Contemporary, Holocene and Quaternary deformation of the Asal rift, Djibouti – implications for the mechanics of slow spreading ridges. *J. Geophys. Res.*, 96, 21789-21806.

Tapponnier, P., R. Armijo, I. Manighetti, and V. Courtillot (1990), Bookshelf faulting and horizontal block rotations between overlapping rifts in southern Afar, *Geophys. Res. Lett.*, 17, 1-4.

Vernant, P., F. Nilforoushan, D. Hatsfeld, M. Abassi, C. Vigny, F. Masson, H. Nankali, J. Martinod, A. Ashtiani, F. Tavakoli, and J. Chéry (2004), Contemporary crustal deformation and plate kinematics in Middle East constrained by GPS measurements in Iran and northern Oman, *Geophys. J. Int.*, 157, 381-398, doi:10;1111/j.1365-246x.2004.02222.x 2004.

Vigny, C., P. Huchon, J.C. Ruegg, K. Khanbari, and L. Asfaw (2006), Confirmation of Arabia plate slow motion by new GPS data in Yemen. *J. Geophys Res.*, 111, B02402, doi:10.1029/2004JB003229.

Walpersdorf A., C. Vigny, J.-C. Ruegg, P. Huchon, L. M. Asfaw and S. Al Kirbash (1999), 5 Years of GPS Observations in the Afar Triple Junction Area, *Journal of Geodynamics*, 28, 2-3, 225-236.

			Horizontal Velocities				Vertical	Velocity uncertainties (1s)			
SITE	Position		/ ITRF2000		/ Somalia						
	Long.	Lat.	East	North	East	North		East	North	Up	Correl.
ARO0	42.85	11.53	33.1	16.2	2.7	0.7	-4.8	0.7	0.7	0.8	-0.004
AS00	42.46	11.64	35.5	14.1	5.0	-1.5	11.7	1.1	1.0	1.4	0.000
BY00	42.54	11.59	49.5	25.0	13.0	9.4	2.7	1.3	1.0	1.9	0.012
CBL0	43.07	11.46	29.4	16.1	-1.0	0.6	-1.7	0.7	0.6	0.9	0.001
CCC0	42.43	11.54	31.4	15.8	0.9	0.2	6.1	0.8	0.7	1.2	-0.047
CF00	42.49	11.62	35.1	23.7	4.7	8.1	4.4	0.9	0.7	1.2	0.012
DF00	42.52	11.60	39.4	24.9	9.0	9.3	7.1	0.9	0.8	1.1	0.043
EP00	42.50	11.57	35.6	16.2	5.2	0.6	1.4	1.0	0.8	1.4	0.026
FFF0	42.52	11.65	40.8	28.0	10.3	12.4	10.6	1.1	1.0	1.7	0.007
FG00	42.47	11.58	30.4	16.6	-0.1	1.0	16.5	4.0	1.4	5.6	0.267
GK00	42.47	11.60	38.5	16.7	8.0	1.0	-11.1	3.0	1.1	3.5	-0.086
GM00	42.56	11.62	41.8	25.4	11.3	9.9	5.4	0.9	0.7	1.2	0.020
GOR0	42.22	11.31	31.1	16.1	0.7	0.4	-8.0	0.9	0.7	1.7	0.002
HD00	42.50	11.61	32.9	18.7	2.5	3.1	1.5	1.7	1.5	3.4	0.007
HM00	42.50	11.55	36.9	16.5	6.5	0.8	19.0	4.6	2.2	8.4	0.168
HX00	42.43	11.59	36.3	19.6	5.9	3.9	5.0	1.3	1.0	2.3	0.021
III0	42.56	11.47	40.1	17.6	9.7	2.0	6.8	1.3	1.0	2.1	0.003
LLL0	42.58	11.26	30.3	15.6	-0.4	-0.2	-2.0	0.7	0.6	0.9	-0.002
LS00	42.52	11.57	36.7	15.6	6.3	0.0	-2.1	0.9	0.7	1.5	0.020
MMM0	42.58	11.62	42.1	26.3	10.7	10.7	6.9	1.1	0.8	2.2	0.009
PPP2	42.64	11.75	41.3	25.6	10.8	10.1	1.3	2.2	1.3	5.4	0.098
QQQ0	42.63	11.44	33.7	16.7	3.2	1.2	1.9	0.8	0.7	1.4	0.008
RRR0	42.67	11.58	43.9	26.6	13.5	11.1	3.3	1.4	1.0	2.8	-0.308
RSB0	43.36	11.98	36.7	24.6	6.1	9.3	0.8	0.8	0.7	1.8	-0.010
SAD0	42.69	11.61	39.1	19.8	8.6	4.3	9.5	2.2	1.5	4.4	0.021
SN00	42.52	11.59	39.1	16.4	8.7	0.8	4.0	1.5	1.1	3.2	0.079
TDJ0	42.91	11.79	36.9	24.2	6.4	8.7	-2.1	0.9	0.8	1.4	-0.024
ADD1	38.77	9.04	25.3	16.5	-4.4	-0.3	-0.5	0.7	0.7	0.8	0.002
DHAM	44.39	14.58	35.6	28.0	4.4	13.0	-1.9	0.8	0.7	1.3	-0.016
HODD	42.97	14.79	35.3	26.8	4.2	11.3	-4.5	1.0	0.8	1.9	-0.053
JNAR	43.44	13.32	37.2	26.7	6.3	11.4	-5.7	1.3	0.8	2.9	-0.067
SANA	44.19	15.35	37.0	26.5	5.6	11.4	-1.1	0.8	0.7	0.9	-0.013

Table 1: Site positions and velocities in ITRF2000 and relative to Somalia plate. Latitude and longitude are in decimal degrees. All velocities and velocity uncertainties are in mm/yr.

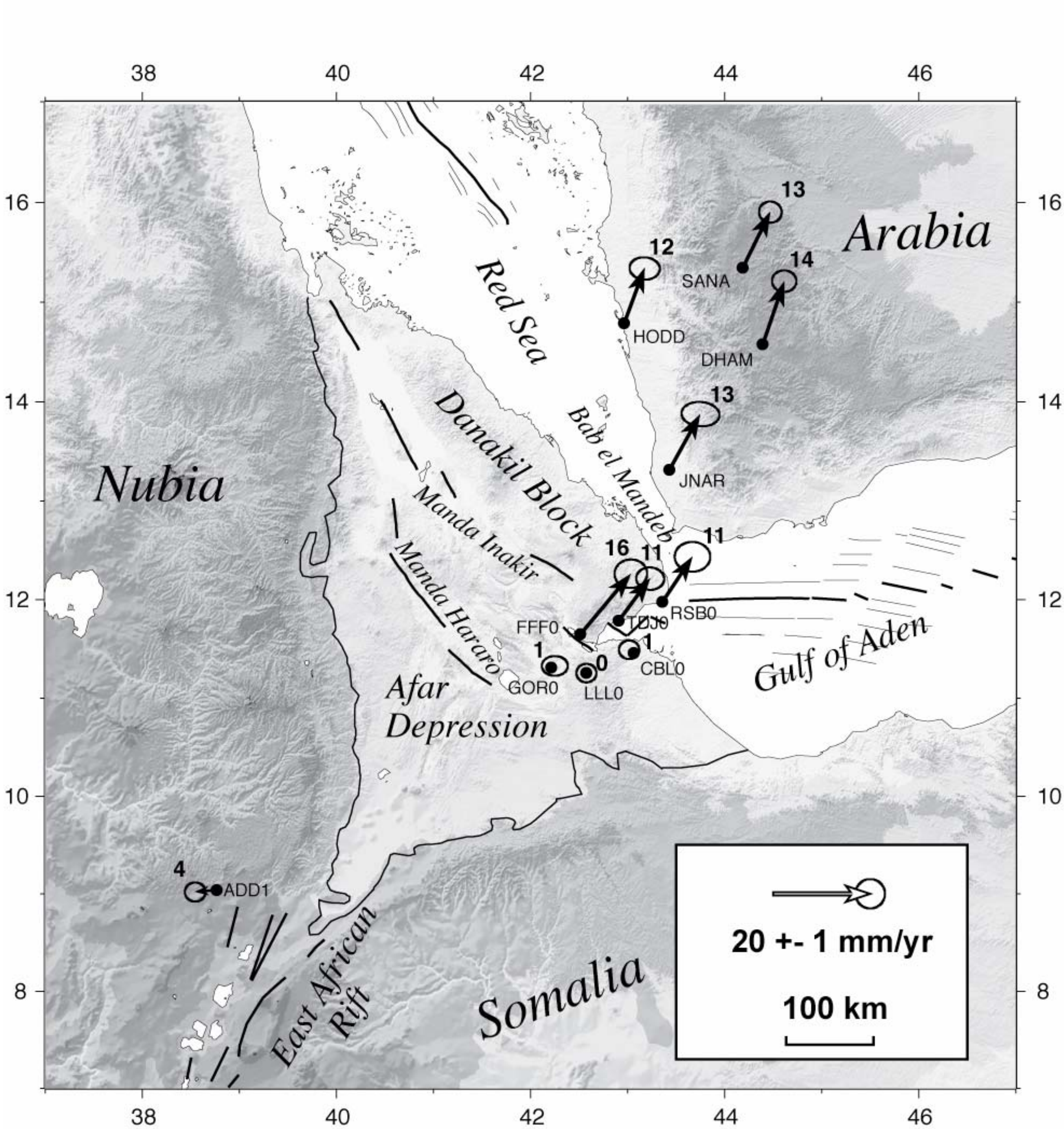

Figure 1. Triple junction and Afar depression. Dots show locations of GPS stations. Arrows depict their horizontal velocities with respect to a reference frame fixed on the Somalia Plate. Bold numbers aside the arrows indicate the velocity in mm/yr. Ellipses depict the region of 99% confidence using the uncertainties in Table 1.

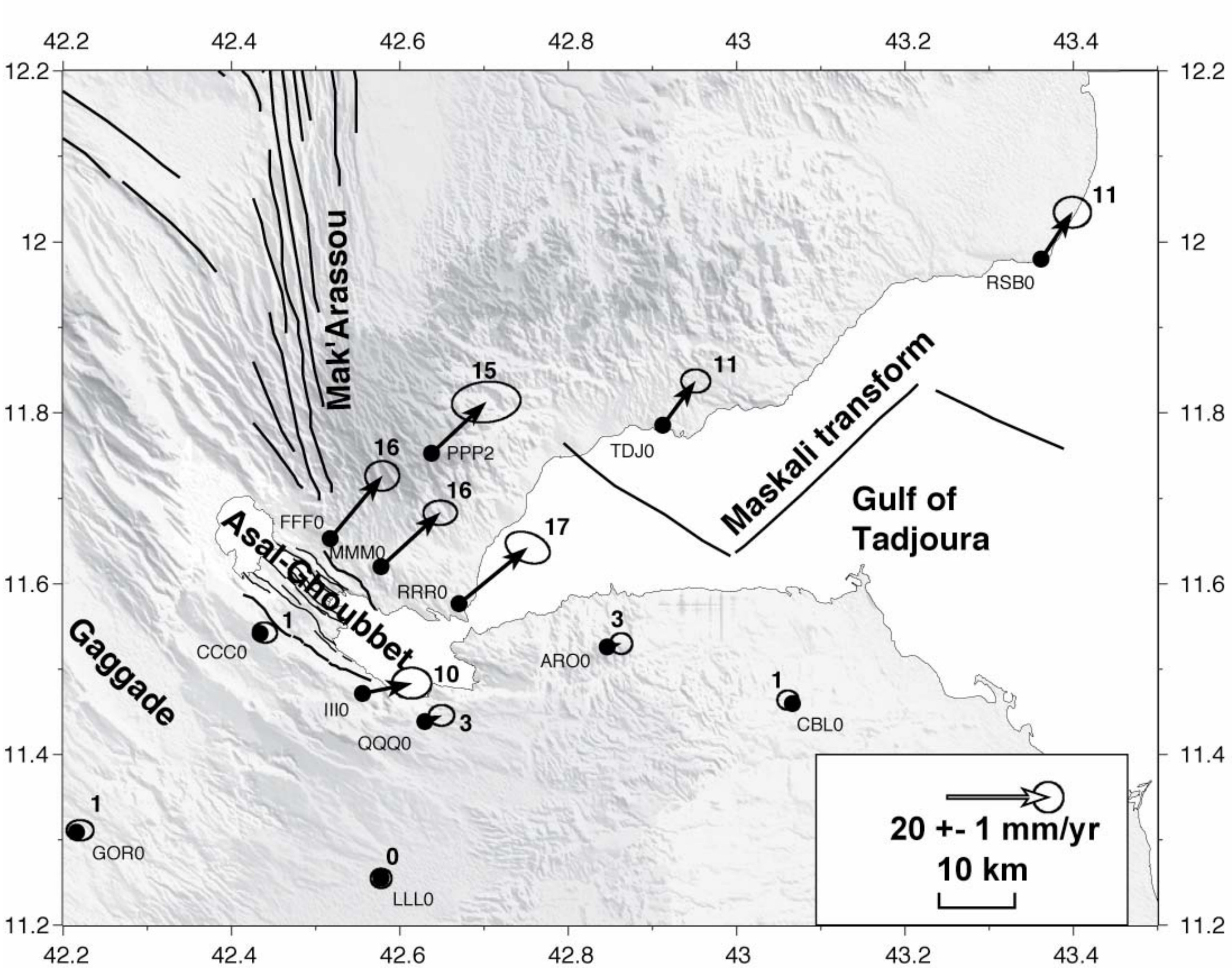

Figure 2. Djibouti and Gulf of Tadjoura. Dots show locations of GPS stations. Arrows depict their horizontal velocities with respect to a reference frame fixed on the Somalia plate. Bold numbers aside the arrows indicate the velocity in mm/yr. Ellipses depict the region of 99% confidence using the uncertainties in Table 1. Thick black lines show the principal directions of active rifting (Mak'Arassou. Asal-Ghoubbet. Gulf of Tadjoura) and the Maskali transform fault. Thin grey lines depict faults in the Asal-Ghoubbet rift.

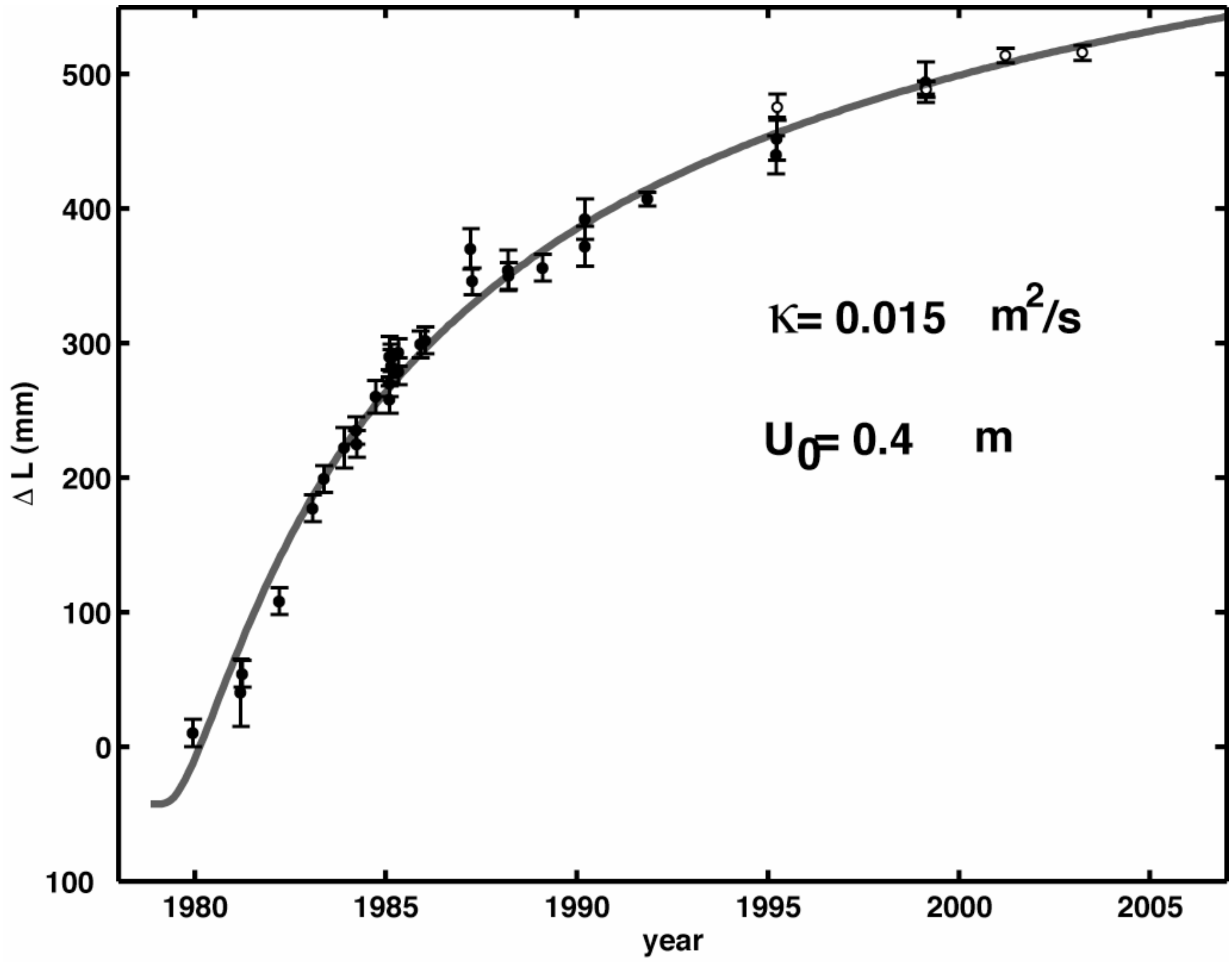

Figure 3. Time-dependent opening of the rift following the 1978 rifting event. The dots show the distance between stations EP00 and DF00 on opposite sides of the rift (see Figure 4 for location). Black symbols depict range measurements. Open symbols denote GPS measurements (since 1995). The vertical bars show one standard deviation for each measurement. The dark line is the best-fitting curve calculated from the diffusive elastic-over-viscous model.

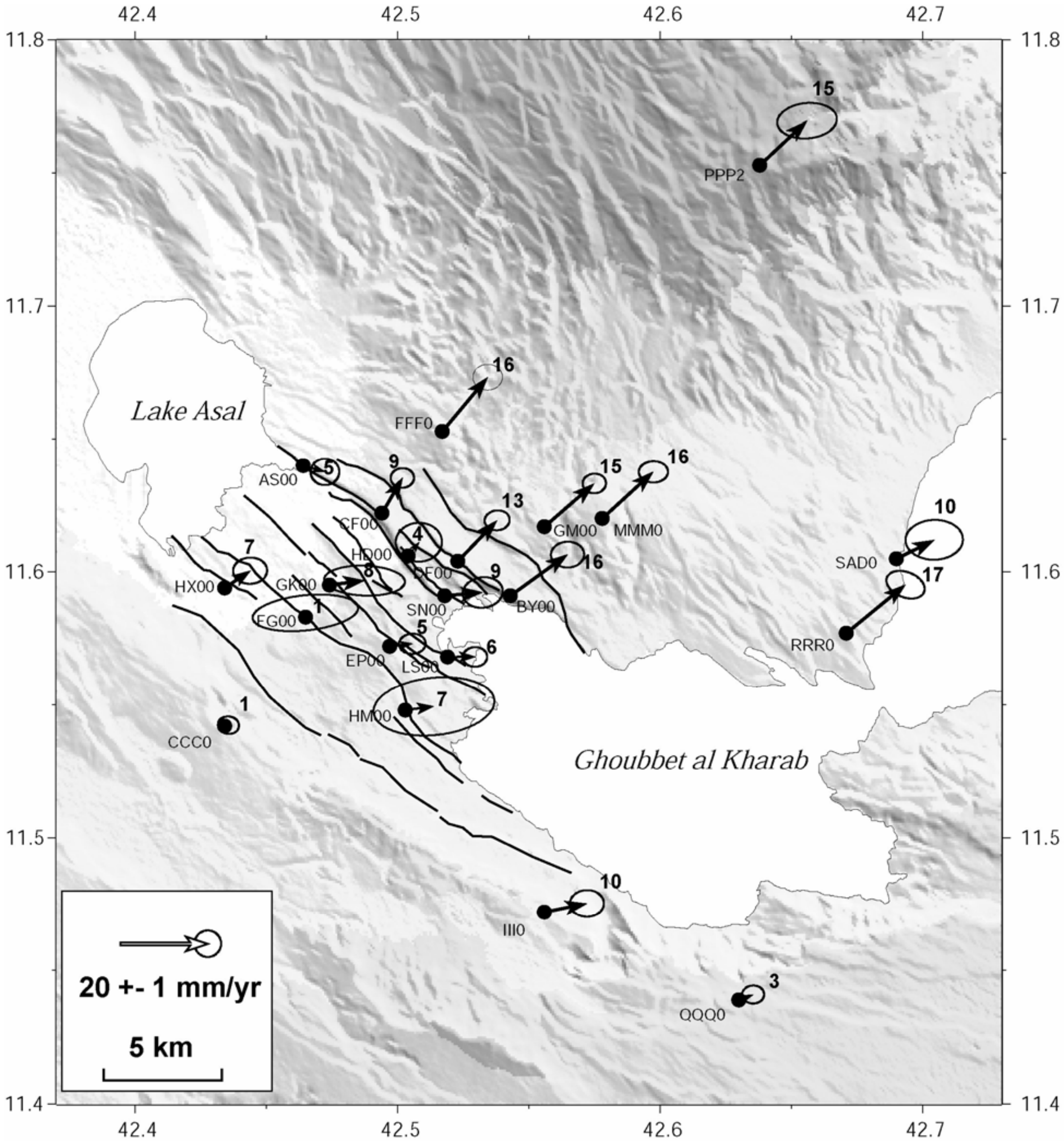

Figure 4: Asal rift. Dots show locations of GPS stations. Arrows depict their horizontal velocities with respect to a reference frame fixed on the Somalia plate. Bold numbers aside the arrows indicate the velocity in mm/yr. Ellipses depict the region of 99% confidence using the uncertainties in Table 1. Black lines show the main active faults in the Asal rift.

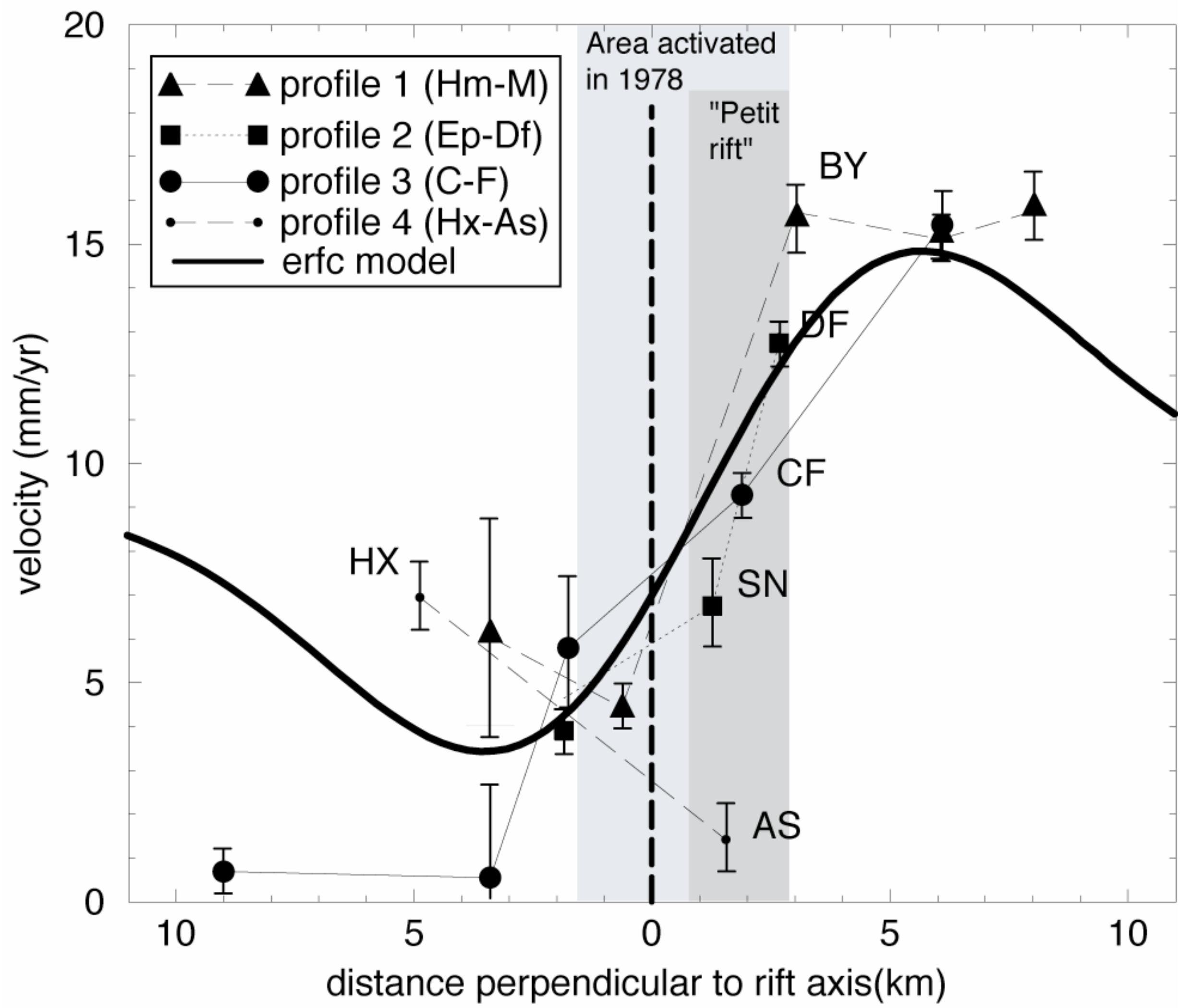

Figure 5: Horizontal velocity components for stations in the Asal rift plotted along profiles perpendicular to the rift axis. The thick dashed line show the rift axis. Rectangular shaded areas indicate the extents of the 1978 rifting event (light) and the “Petit Rift” (dark). The thick black curve depicts the Erfc elastic-over-viscous model computed with the parameters inferred from model curve in Figure 3 and t=19 years since 1978 and centered at +1 km. Triangles and dashed line depict the first profile near Ghoubbet (HM00 – LS00 – BY00 – GM00 – MMM0). Squares and dotted line depict the second profile (EP00 – SN00 – DF00). Circles and full line depict the third profile near lake Asal (CCC0 – FG00 – GK00 – CF00 – FFF0). Dots and long dashed line depict the last 2 points at lake Asal (HX00 – AS00). Error bars represent the 1-sigma uncertainties of Table 1.

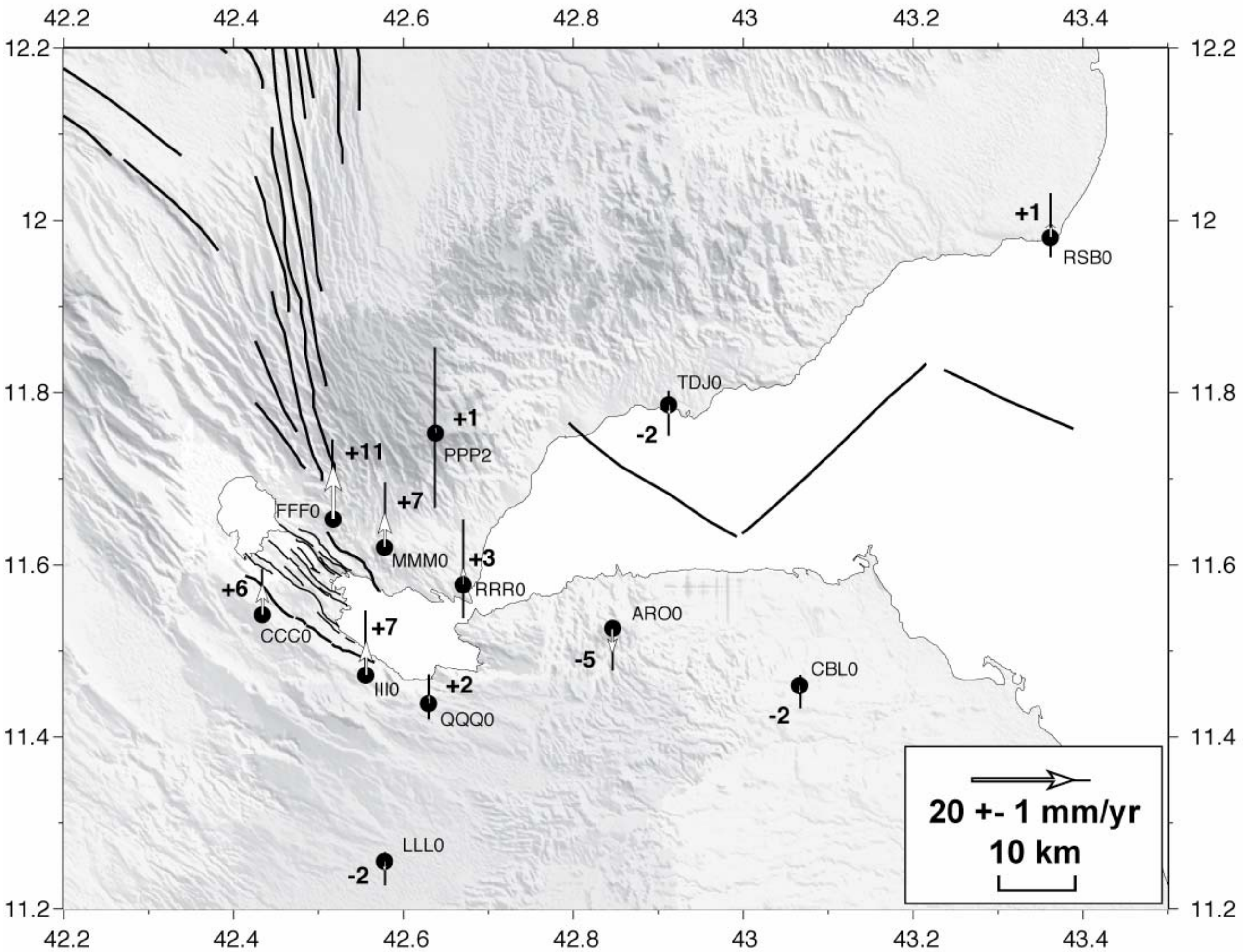

Figure 6. Vertical velocities in Djibouti. Dots show locations of GPS stations measured at least 3 times. Arrows depict the GPS vertical velocities at those locations: arrows pointing North indicate upward velocities. Numbers beside the arrow heads indicate the velocity in mm/yr. Vertical thin lines at the arrow heads give the 99% confidence level using uncertainties from Table 1.

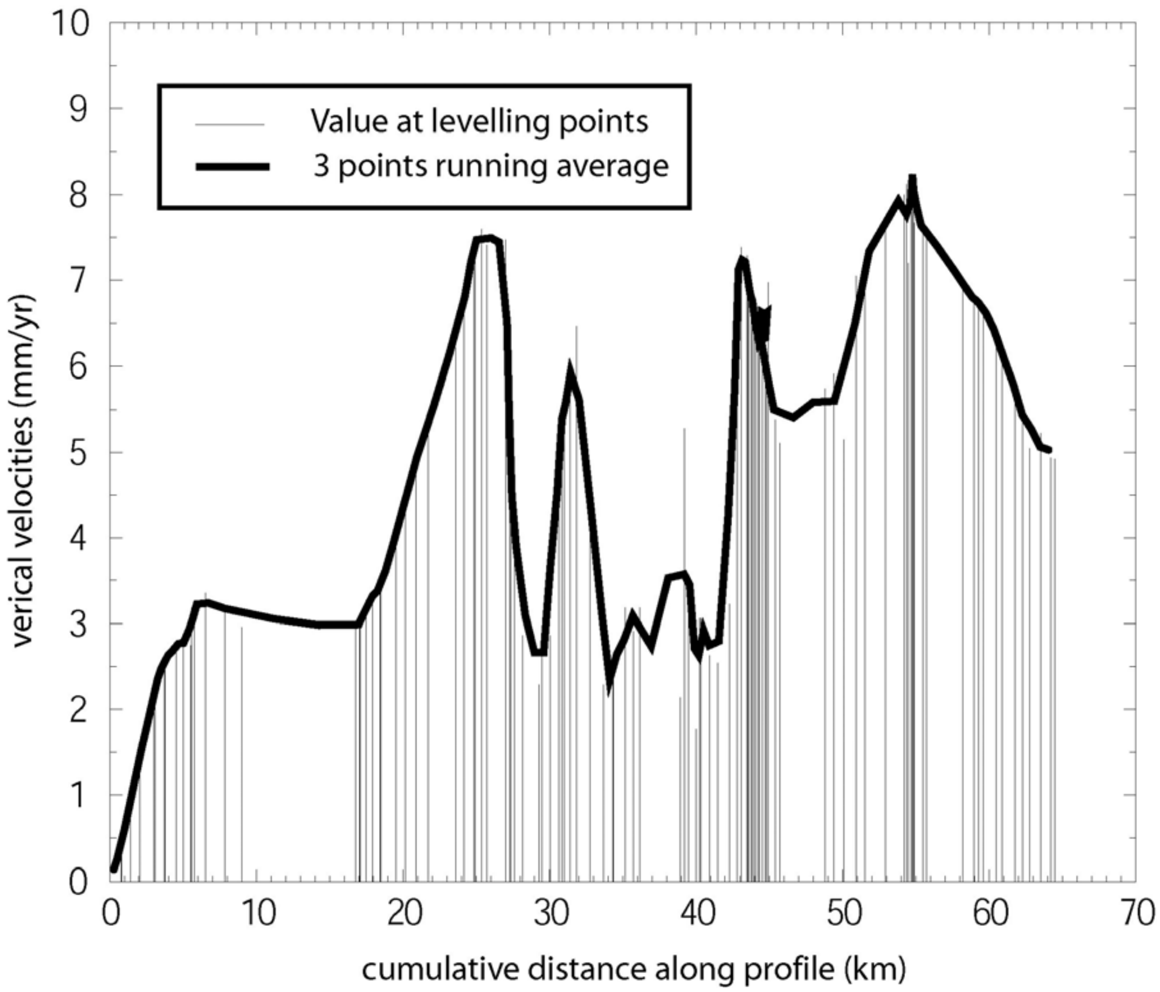

Figure 7: Leveling profile velocities (2000 – 1985) projected on an axis perpendicular to the rift (strait grey line on Figure 8). The vertical thin lines indicate the difference between 2000 and 1985 measurement at each benchmark of the profile. The thick curve is a 3-point running average of these measurements.

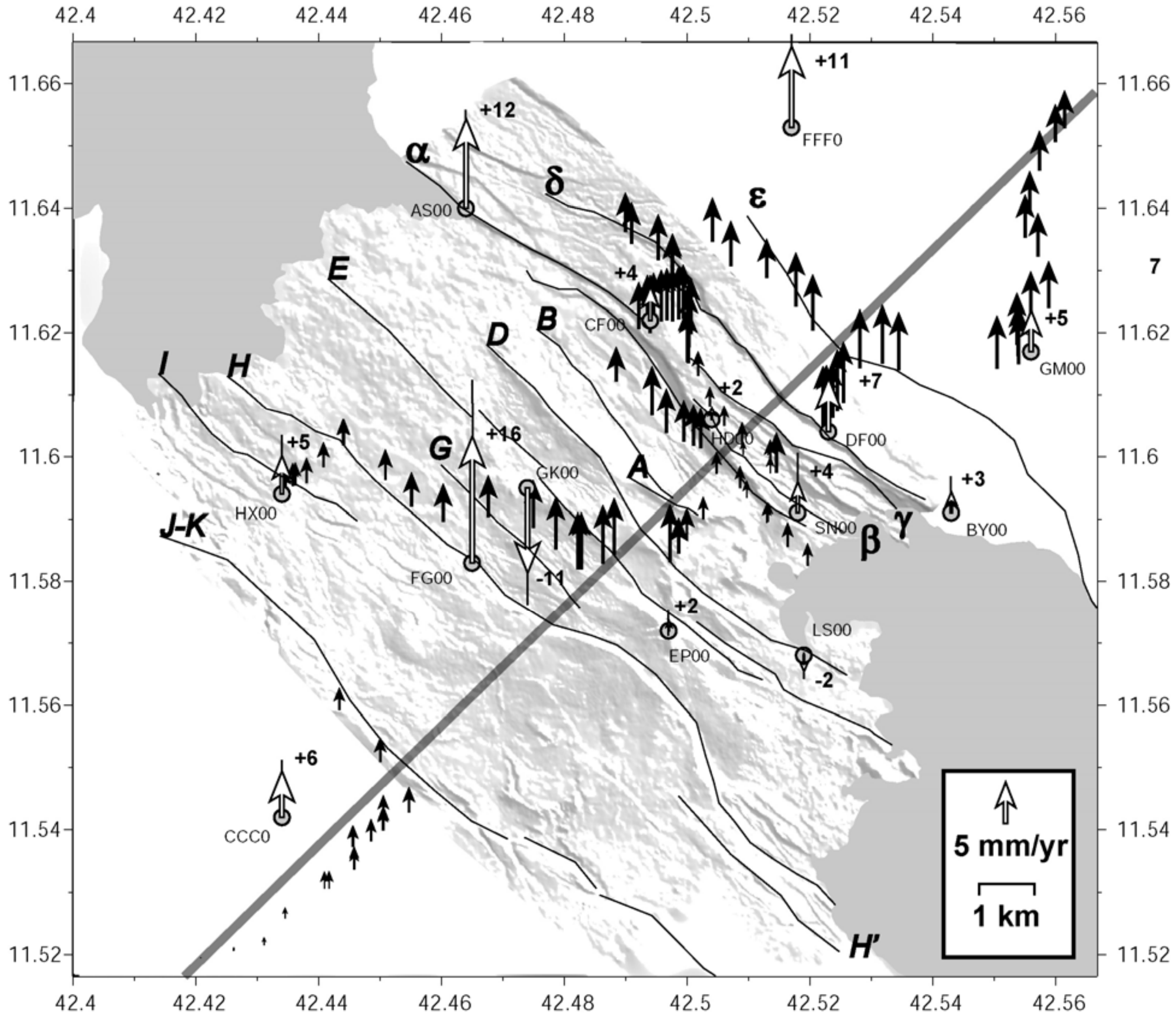

Figure 8: Vertical velocities inside the Asal rift. Dots show locations of GPS stations. Open arrows depict the GPS vertical velocities. Dark arrows depict the velocities obtained from leveling profiles. Arrows pointing North indicate upward velocities. Vertical thin lines at the arrow heads give the 99% confidence level using Table 1 vertical velocity uncertainty (no uncertainties for the leveling velocities). Bold numbers aside the arrowheads indicate the velocity in mm/yr. Grey line shows the direction along which the 1D profile of Figure 7 is plotted. The background topography is from the 10 m-resolution digital elevation model made from aerial photography [*de Chabalier and Avouac*, 1994]. Fault labels (A-K and α−ε) are from *Stein et al.* [1991].

Supplementary material, to be published as an electronic supplement (Table S1, figure S1)

SITE	1991	1993	1995	1997	1999	2001	2003
ARO0	**45** AL12-L12	**25** TSST-SST AP12-P12	**13** AZ12-GD3	**11** AZ12-GD3	**14** AZ12-DMG	**14** AZ12-DMG	**13** AZ12-GD3
AS00					**2** AZX-DMG	**5** AZX-DMG	**10** AZX-GD4
BY00			**1** AZ12-P12		**2** AZ12-DMG		**3** AZX-GD4
CBL0	**8** AL12-L12		**1** AZ12-P12		**2** AZ12-DMG	**2** AZX-DMG	**2** AZX-GD4
CCC0	**3** AL12-L12				**3** AZX-DMG	**2** AZ12-DMG	**6** AZX-GD4
CF00			**1** AZ12-P12		**5** AZX-DMG	**5** AZ12-DMG	**4** AZX-GD4
DF00			**3** AZ12-P12		**10** AZX-DMG	**9** AZX-DMG	**12** AZX-DMG
EP00			**3** AZ12-L12		**5** AZ12-DMG	**6** AZX-DMG	**4** AZX-GD4
FFF0	**2** TSST-SST				**2** AZX-DMG	**1** AZX-MRA	**3** AZX-GD4
FG00			**1** AZ12-P12		**1** AZX-DMG		**2** AZX-GD4
GK00			**1** AZ12-P12		**1** AZX-DMG	**1** AZ12-DMG	
GM00			**2** AZ12-P12		**4** AZ12-DMG	**2** AZX-DMG	**4** AZX-GD4
GOR0	**3** AL12-L12 TSST-SST						**1** AZX-GD4
HD00						**2** AZX-DMG	**2** AZX-GD4
HM00						**1** AZ12-DMG	**2** AZX-GD4
HX00			**1** AZ12-P12		**2** AZX-DMG	**1** AZ12-DMG	**2** AZX-GD4
III0	**1** TSST-SST				**2** AZX-DMG	**2** AZ12-DMG	**2** AZX-GD4
LLL0	**16** TSST-SST AL12-L12	**3** AP12-P12	**2** AZ12-P12	**1** AZ12-GD3	**2** AZ12-DMG	**2** AZ12-MRA	**3** AZX-GD4
LS00			**1** AZ12-P12		**1** AZ12-DMG	**3** AZ12-DMG	**3** AZX-GD4
MMM0	**2** TSST-SST AL12-L12				**2** AZX-DMG	**2** AZ12-DMG	**2** AZX-GD4
PPP2	**1** AL12-L12						**1** AZX-GD4
QQQ0	**6** AL12-L12		**1** AZ12-P12		**2** AZX-DMG	**2** AZ12-DMG	**2** AZX-GD4
RRR0	**2** AL12-L12					**2** AZ12-MRA	
RSB0	**9** TSLD-SLD				**2** AZ12-DMG	**2** AZ12-DMG	**4** AZX-GD4
SAD0						**2** AZX-DMG	**2** AZX-GD4
SN00					**1** AZX-DMG	**1** AZ12-DMG	**4** AZX-GD4
TDJ0			**1** AZ12-P12		**2** AZX-DMG	**2** AZ12-DMG	**3** AZX-GD4
ADD1	**20** AL12-L12		**9** TSSE-SST	**7** TSSE-SST	**13** TSSE-SST	**13** TSSE-SST	**14** TSSE-SST
DHAM	**4** AL12-L12					**3** AZ12-P12	
HODD	**3** AL12-L12					**3** AZ12-P12	
JNAR	**2** AL12-L12					**2** AZ12-P12	
SANA	**15** AL12-L12	**26** AP12-P12	**9** AP12-P12		**12** AZ12-P12	**9** AZ12-P12	

Table S1: Site occupations. Bold numbers indicate the number of sessions at each site. The following codes indicate the type of equipment used. Receivers are Trimble 4000 SLD (TSLD) or SST (TSST); or Ashtech codeless L2 (AL12). P-code L2 (AP12). Z-tracking (AZ12). micro-Z (AZX). Antennas are Trimble SLD (L1/L2 4000 model 12562 - square ground plane) or SST (L1/L2 4000 model 14532 – round ground plane); or Ashtech L12 (geodetic L1/L2 type 1 - closed holes on ground plane – IGS#:

ASH700228A). P12 (geodetic L1/L2 type 2 - open holes on ground plane – IGS#: ASH700228D). GD3 (geodetic L1/L2 type 3 - large ground plane "whopper" – IGS#: ASH700718A). MRA (dual frequency marine – IGS#: 700700.A). DMG (Dorne-margolin "choke ring" – IGS#: ASH700936A) or GD4 (geodetic type 4 - small antenna without ground plane –IGS#: ASH701975.01A).

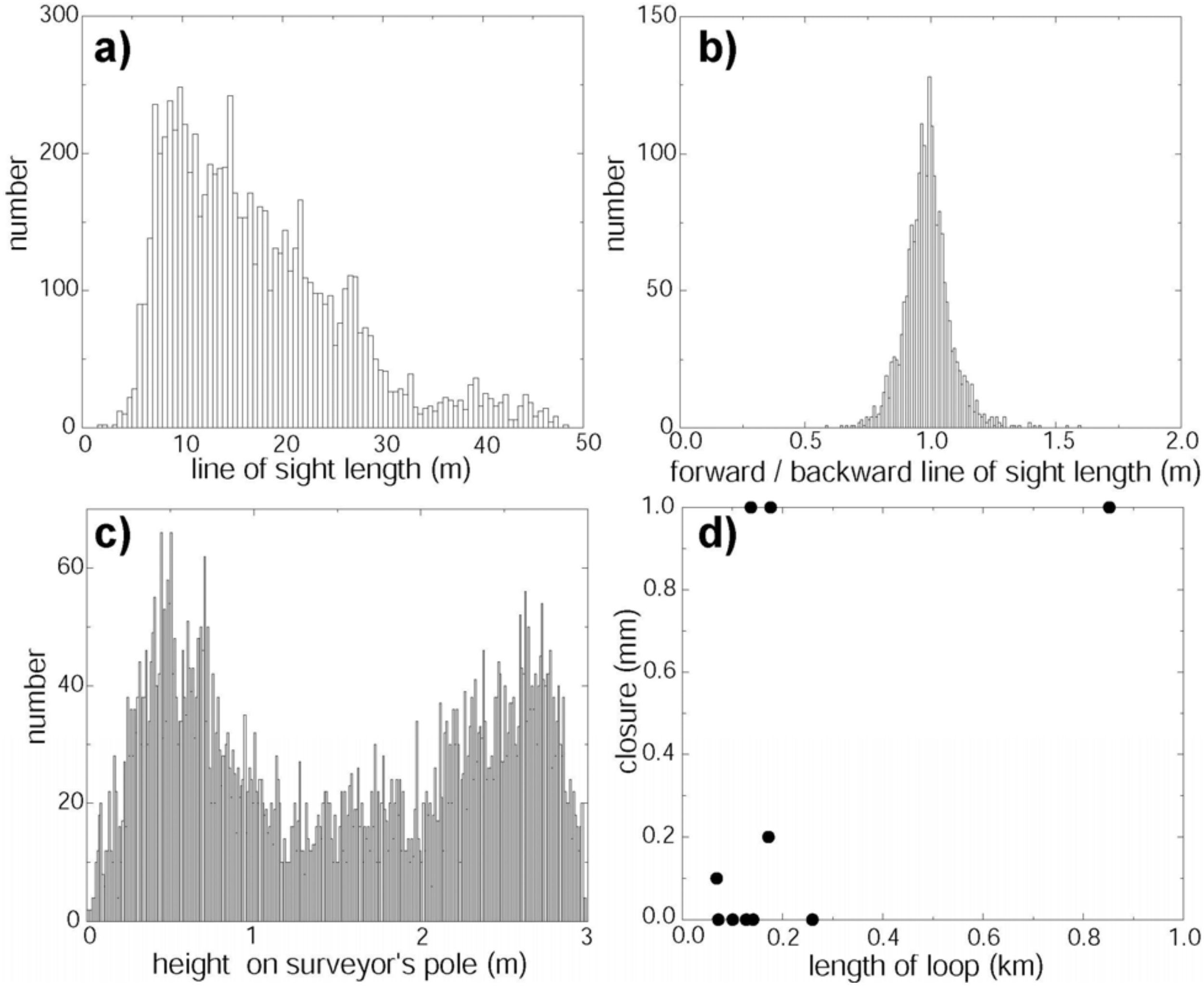

Figure S1: Leveling profile technical characteristic and quality assessment. Histograms of: (a) length of line of sights; (b) ratio of forward and backward line of sight lengths; (c) heights hit on the surveyor's pole; and (d) misclosure of small loops.